HHS Public Access

Author manuscript

Neuroscience. Author manuscript; available in PMC 2017 March 11.

Published in final edited form as:

Neuroscience. 2016 March 11; 317: 1–11. doi:10.1016/j.neuroscience.2015.12.054.

Changes in the Disposition of Substance P in the Rostral Ventromedial Medulla after Inflammatory Injury in the Rat

Uche P. Maduka[a], **Marta V. Hamity**[b], **Roxanne Y. Walder**[b], **Stephanie R. White**[b], **Yalan Li**[c], and **Donna L. Hammond**[a,b]

[a]Department of Pharmacology, Carver College of Medicine, University of Iowa, Iowa City, IA 52242

[b]Department of Anesthesia, Carver College of Medicine, University of Iowa, Iowa City, IA 52242

[c]Department of Proteomics Core Facility, Carver College of Medicine, University of Iowa, Iowa City, IA 52242

Abstract

This study examined whether peripheral inflammatory injury increases the levels or changes the disposition of substance P (SubP) in the rostral ventromedial medulla (RVM), which serves as a central relay in bulbospinal pathways of pain modulation. Enzyme immunoassay and reverse transcriptase quantitative polymerase chain reaction were used to measure SubP protein and transcript, respectively, in tissue homogenates prepared from the RVM and the periaqueductal gray and cuneiform nuclei of rats that had received an intraplantar injection of saline or complete Freund's adjuvant (CFA). Matrix Assisted Laser Desorption/Ionization Time of Flight analysis confirmed that the RVM does not contain hemokinin-1, which can confound measurements of SubP because it is recognized equally well by commercial antibodies for SubP. Levels of SubP protein in the RVM were unchanged four hours, four days and two weeks after injection of CFA. *Tac1* transcripts were similarly unchanged in the RVM four days or two weeks after CFA. In contrast, the density of SubP immunoreactive processes in the RVM increased 2-fold within four hours and 2.7-fold four days after CFA injection; it was unchanged at two weeks. SubP-immunoreactive processes in the RVM include axon terminals of neurons located in the periaqueductal gray and cuneiform nucleus. Substance P content in homogenates of the periaqueductal gray and cuneiform nucleus was significantly increased four days after CFA, but not at four hours or two weeks. *Tac1* transcripts in homogenates of these nuclei were unchanged four days and two weeks after CFA. These findings suggest that there is an increased mobilization of SubP within processes in the RVM shortly after injury accompanied by an increased synthesis of SubP in neurons that project to the RVM. These findings are consonant with the hypothesis that an increase in SubP release in the RVM contributes to the hyperalgesia that develops after peripheral inflammatory injury.

Address correspondence to: Donna L. Hammond, PhD, University of Iowa, 3000 ML, Iowa City, IA 52242, 319-335-9595 (voice), donna-hammond@uiowa.edu.

Drs. Maduka and Hamity share first authorship

Keywords

Substance P; rostral ventromedial medulla; hemokinin-1; neurokinin-1 receptor; hyperalgesia; inflammation

INTRODUCTION

Substance P (SubP) is acknowledged to play an important role in inflammatory nociception. The mechanisms by which it acts in the periphery and spinal cord to induce and maintain heat hyperalgesia and mechanical hypersensitivity after peripheral inflammatory injury are well characterized (see reviews by (Baranauskas and Nistri, 1998; Sandkuhler et al., 2000; Snijdelaar et al., 2000; Mantyh, 2002; Keeble and Brain, 2004; Seybold, 2009; Todd, 2010; Steinhoff et al., 2014). Our understanding of its actions within supraspinal nuclei that modulate the transmission of nociceptive information in the spinal cord continues to evolve, particularly with respect to its actions in the rostral ventromedial medulla (RVM) (Lagraize et al., 2010; Hahm et al., 2011; Brink et al., 2012; Khasabov and Simone, 2013; Hamity et al., 2014).

The RVM, which contains the nucleus raphe magnus and nucleus reticularis gigantocellularis, serves as a central relay in the bulbospinal pathways that can both facilitate and suppress nociceptive transmission within the dorsal horn of the spinal cord (Millan, 2002; Heinricher et al., 2009). The RVM contains high concentrations of SubP that originate from neurons located in the nucleus cuneiformis, dorsal raphe nucleus, and periaqueductal gray (PAG) (Beitz, 1982; Chen et al., 2013), as well as a moderate density of neurokinin-1 receptors (NK1R) at which SubP exerts its actions (Saffroy et al., 1988; Nakaya et al., 1994; Hamity et al., 2014). In uninjured animals, a single injection or continuous infusion of SubP into the RVM causes hypersensitivity of the hindpaw to noxious heat stimuli that can last 24 hours (Hamity et al., 2010; Lagraize et al., 2010). Microinjection of NK1R antagonists into the RVM of animals with inflammatory injury induced by capsaicin or complete Freund's adjuvant (CFA) prevents and reverses thermal hypersensitivity, while in uninjured animals, delivery of these same NK1R antagonists into the RVM does not interfere with their normal behavioral responsiveness to thermal or mechanical stimuli (Pacharinsak et al., 2008; Hamity et al., 2010; Lagraize et al., 2010; Brink et al., 2012). Chemical ablation of NK1R in the RVM also blocks thermal and mechanical sensitivity following capsaicin and CFA-induced inflammation (Khasabov and Simone, 2013). These data collectively implicate SubP in the RVM in the development and maintenance of a persistent pain state after peripheral inflammatory injury.

There are many mechanisms by which SubP can function within the RVM to modulate nociception. Previous work documented that NK1R is upregulated in the RVM as early as two hours to four days after peripheral inflammatory injury (Lagraize et al., 2010; Hamity et al., 2014). Also, the number of neurons that express NK1R is increased four days after intraplantar injection of CFA (Hamity et al., 2014). However, whether a corresponding increase in the levels or change in the disposition of SubP, the endogenous ligand for NK1R, occurs in the RVM following inflammatory injury is unknown. This study therefore

examined levels of *Tac1* transcript and SubP protein in the RVM and PAG and adjacent cuneiform nuclei at various times after intraplantar injection of CFA. It also determined whether hemokinin-1 (HK-1) transcript or protein is present in the RVM. This latter set of experiments was driven by the disclosure that the antibody in the enzyme immunoassay (EIA) kit used to quantitate SubP also recognizes HK-1, the product of the *Tac4* gene, with equal affinity. The amino acid sequences for SubP and HK-1 are 55% identical, and both proteins bind the NK1R with similar high affinity (Morteau et al., 2001; Camarda et al., 2002; Duffy et al., 2003; Berger and Paige, 2005). The potential presence of HK-1 was a confound not only for the specificity of the EIA, but also because HK-1 is upregulated in glia by inflammatory stimuli (Morteau et al., 2001; Duffy et al., 2003; Fu et al., 2005; Endo et al., 2006; Matsumura et al., 2008) and has recently been implicated in nociception or itch (Funahashi et al., 2014) and in CFA-induced chronic arthritis (Borbely et al., 2013).

EXPERIMENTAL PROCEDURES

Animals

These studies were approved by the University of Iowa Animal Care and Use Committee (protocol #1106133) and were conducted in accordance with the guidelines set forth by the National Institutes of Health and the International Association for the Study of Pain. Every effort was made to minimize animal suffering and the number of animals used in this study. Male Sprague Dawley rats weighing 225 – 250 g (Charles River Laboratories, Raleigh, NC) were purchased for this study. All rats were allowed to acclimate at least 48 hours in the University of Iowa Animal Care facility prior to any experiment. Rats were housed in the animal care facility as two per cage in a temperature and humidity controlled room with a 12 hour light/dark cycle, and access to food and water was provided *ab libitum*.

Model of inflammatory pain

The CFA-induced model of inflammatory injury has been previously described (Hurley and Hammond, 2000; Sykes et al., 2007; Hamity et al., 2010). Briefly, rats were weighed and lightly anesthetized with isoflurane. The distance between the dorsal and ventral surfaces (thickness) of each hind paw was measured using digital calipers; then the plantar surface of the left hindpaw was injected with 0.15 ml CFA (150 μg of *Mycobacterium butyricum*, 85% Marcol 52, and 15% Aracel A mannide monoemulsifier) (Calbiochem, San Diego, CA) or 0.15 ml sterile-filtered saline (pH 7.4). After intraplantar injection, the rats were singly housed. Four hours, four days, and two weeks were selected to represent the acute, subacute, and chronic phases of inflammatory injury, in accordance with previous studies. At the designated time points, the rats were weighed and the thickness of their hindpaws was measured to assess the extent of the inflammation.

Measurement of heat hyperalgesia

Thermal sensitivity was measured as previously reported by our group (Hurley and Hammond, 2000). Briefly, at the corresponding times after saline or CFA treatment, the rats were acclimated to the testing room for 30 min then placed in individual Plexiglas chambers on a 25°C glass surface for another 30 min of acclimation. Sensitivity to noxious heat was measured by focusing a high-intensity beam of light on the plantar surface of the hindpaw.

The time required for the rat to withdraw its hindpaw from the heat stimulus was automatically measured and recorded as the paw withdrawal latency (PWL). Baseline PWL was typically 8 to 12 s. To prevent tissue damage, the maximum time of exposure to the light beam was 20 s.

Analysis of *Tac1* and *Tac4* mRNAs

Tissue collection—Punches containing the RVM and the combination of PAG and cuneiform nuclei were collected from animals at four days or two weeks after saline or CFA injection in the hindpaw. The thickness of the hindpaw was measured prior to euthanasia. Nociceptive behavior tests were not conducted on rats used for qPCR experiments. Each group contained 6-8 animals. The rats were euthanized with CO_2 exsanguinated, and brains were quickly removed. A 2-mm thick coronal block of the brainstem 3 and 5 mm rostral to the obex, which contains the RVM, was immediately dissected on ice and frozen on a platform on dry ice. One 1.5 mm diameter tissue punch (Harris Unicore, Ted Pella Inc., Redding, CA), centered on the midline immediately above the pyramids, was removed from the frozen brainstem tissue and placed in RNAlater™ (Ambion, Life Technologies, Carlsbad, CA). The brain slices then were fixed in 10% formalin containing 30% sucrose so the location of the tissue punch could be verified. The PAG tissue was dissected from a frozen 2-mm transverse slice of the midbrain between the locus coeruleus and the inferior colliculus. A 2-mm tissue punch was used to obtain the ventrolateral aspects of the ipsilateral and contralateral PAG and cuneiform nucleus, with respect to the injected hindpaw. The tissue was immediately placed in RNAlater™. All tissue samples were stored at −20 °C until RNA isolation. The location and relative size of the tissue punches within the coronal sections of the brainstem were similar to previously published diagrams (Hurley and Hammond, 2000).

RNA isolation, RT, and qPCR—Total RNA was extracted from the RVM and the ipsilateral and contralateral PAG of saline- and CFA-treated rats using the Qiagen RNeasy lipid tissue mini kit (Qiagen, Valencia, CA) as previously described (Hamity et al., 2014). Sufficient quantities of RNA could be isolated from single punches of RVM and PAG tissue for multiple analyses. The RNA purification included an on-column DNAse1 treatment to remove DNA contamination. RNA concentration and purity were assessed by spectrometry (Nanodrop, Thermo-Scientific, Wilmington, DE). As a means of quality control, RNA integrity analysis was determined on 20% of the samples and consistently yielded a value >9 (out of 10) (Agilent 2100 bioanalyzer, Agilent Technologies; Santa Clara, CA). Reverse transcription (RT) was performed using 50 ng of purified RNA and the SuperScript VILO cDNA synthesis kit (Invitrogen, Carlsbad, CA) in a 20 μl reaction volume at 42° for 1 hour. PCR was performed in triplicate using 2 μl of the RT product (5 ng) in a 20 μl reaction volume with primers complementary to rat *Tac1* (SubP), *Tac4* (HK-1), *Actb* (β-actin), or *Mapk6* (mitogen-activated protein kinase 6) and IQ Sybr Green Supermix (Bio-Rad, Hercules, CA). No reverse transcriptase and no template controls were also run in triplicate. Cycle conditions were 50 °C for 2 min, 95 °C for 10 min, 40 cycles of 95 °C for 15 sec, 60 °C for 1 min, and 72 °C for 1 min. Since both of the *Tac1* and *Tac4* genes have several splice variants (Steinhoff et al., 2014), the primers were designed to detect mRNAs containing the sequences of the mature neuropeptides. *Actb* and *Mapk6* were used as

reference genes. Table 1 lists the primers and sizes of the PCR products. All primers were designed to span introns to exclude genomic DNA contamination. The amplification efficiency of the *Tac1* assay was 100%, r^2= 0.998, slope = −3.270 and of the *Tac4* assay, efficiency = 97.4%, r^2 = 0.997, slope = −3.386. The amplification efficiency of the *Actb* assay was 100%, r^2 = 0.997, slope = −3.282, and of the *Mapk6* assay was 100%, r^2 = 0.998, slope = −3.215. Cycle thresholds (C_T) for *Tac1*, *Tac4*, *Actb*, and *Mapk6* were converted to absolute copy numbers using standard curves of cloned plasmids containing the amplicons for *Tac1*, *Tac4*, *Actb, and Mapk6*, at 10^6, 10^5, 10^4, 10^3, and 10^2 copies.

For the RVM, the expression of *Tac1* was normalized to *Actb* by calculation of the ΔC_T and then transformation to linear scale as $2^{-\Delta CT}$ for statistical analysis. *Actb* was used as a normalization gene in the RVM because it was stably expressed in all four treatment groups (data not shown), consistent with an earlier report from this laboratory (Walder et al., 2014). For subsequent determination of *Tac1* expression in the PAG, levels of *Tac1* were normalized to the geometric mean of *Actb* and *Mapk6 calculated* as ΔC_T followed by transformation to linear scale as $2^{-\Delta CT}$ for statistical analysis. *Actb* and *Mapk6* were previously validated as reference genes for the RVM (Walder et al., 2014) and confirmed here for the PAG (M values of 0.55 for stability of gene expression) in the CFA model of inflammatory injury.

Enzyme immunoassay of SubP

Tissue collection—RVM tissue was collected from animals four hours, four days or two weeks after injection of saline or CFA in the hindpaw. Prior to euthanasia, PWL to noxious heat stimulation and the thickness of the hindpaws were measured. Each group contained 8-16 animals. After nociceptive behavior testing, the rats were euthanized with CO_2, exsanguinated, and the brains were quickly removed. A 2-mm thick coronal block of the brainstem was taken 3 and 5 mm rostral to the obex. Two tissue punches (0.75 mm diameter) that each abutted the midline over the pyramids were obtained (Harris Unicore, Ted Pella Inc., Redding, CA) from the RVM, one ipsilateral and the other contralateral to the injected hindpaw. Each side of the RVM was analyzed separately. Punches of ipsilateral and contralateral PAG were obtained as described above for the RT-qPCR experiments. The tissue was weighed and samples whose weight was greater or less than 2 SD from the mean were excluded from analysis. These corresponded to one sample in each CFA- and saline-treated treatment group at 4 hrs and 2 weeks for the RVM samples. There were no significant differences in the weight of the tissue punches obtained from saline- and CFA-treated rats at any time point, or between ipsilateral and contralateral sides for either the RVM or PAG tissue samples (P > 0.1 all comparisons).

SubP measurement—RVM and PAG tissue punches were processed immediately after collection. They were mechanically homogenized in 0.5 ml of 2 M acetic acid and then centrifuged at 16,100 *g* for 10 min using an Eppendorf 5415r tabletop centrifuge. The supernatants were carefully removed, lyophilized to dryness using a Savant Speed Vac SC110 (Holbrook, NY), and reconstituted in EIA buffer. SubP concentrations were determined with an EIA kit (Cayman Chemicals, Ann Arbor, MI) as directed by the manufacturer. All samples were diluted to yield SubP concentrations within the linear range

of the standard curve (3.9-500 pg/ml). SubP content was expressed as pg/mg wet tissue weight.

Immunohistochemistry

Antibody characterization—Guinea pig polyclonal SubP antiserum, directed against Cys-Arg-Pro-Lys-Pro-Gln-Gln-Phe-Phe-Gly-Leu-Met, a modification of the rat SubP sequence, was purchased from Neuromics (Edina, MN, GP14103, lot number 401159). The specificity of the antiserum was confirmed by immunolabeling striatum tissue sections from the brains of C57Bl6/J (wild type) and *Tac1* null mice (B6.CGTac1tm1Bbm/J, Jackson Labs, Bar Harbor, ME) for SubP. Dense labeling of the processes in the medial preoptic nucleus adjacent to the third ventricle and the basal nucleus of the striatum was observed in the wild type tissue and there was an absence of labeling in the same region in the *Tac1* null tissue. The secondary antibody, biotinylated donkey anti-guinea pig IgG (706-065-148, lot number 112634), was purchased from Jackson ImmunoResearch (West Grove, PA).

Tissue processing—Cohorts of rats were allocated into six treatment groups: four hour saline, four hour CFA, four day saline, four day CFA, two week saline, and two week CFA. The intraplantar hindpaw injections were timed to allow the rats from different groups to reach the desired time point on the same day. To reduce variability, tissue samples from different treatment groups were processed and stained concurrently. Three to six replicates were completed for this experiment. Nociceptive behavior tests were not conducted on animals used for immunohistochemistry experiments.

To prepare the rats for fixation, the animals were deeply anesthetized with sodium pentobarbital (50 mg/kg, Lundbeck Inc., Deerfield, IL), the chest cavity was exposed and 0.1 ml heparin (1000 USP units, Hospira Inc., Lake Forest, IL) was administered into the heart. Rats were transcardially perfused with 100 ml of 0.9% saline at 37°C, followed by 300 ml of ice cold 4% paraformaldehyde pH 7.4. Following perfusion, the rat brains were removed, post fixed in 4% paraformaldehyde pH 7.4 for 30 min, and placed in 30% sucrose in 0.1 M phosphate buffered saline (PBS) pH 7.4 at 4°C for 48 hrs for cryoprotection.

After cryoprotection, the brainstem was frozen in optimal cutting temperature media (Sakura Finetek, Torrance, CA). Coronal sections of 50-μm thickness were cut through the rostral to caudal extent of the RVM using a cryostat and collected into 0.1 M PBS pH 7.4 as free-floating sections. Serial sections were treated with 1.67% hydrogen peroxide in methanol for 20 min, washed several times with 0.1 M PBS pH 7.4 and then incubated in 1% sodium borohydride for 30 min. Following several washes with 0.1 M PBS pH 7.4, sections were incubated in 2% normal donkey serum (Lampire, Pipersville, PA) with 0.3% Triton X-100 in 0.1 M PBS pH 7.4, which served as the blocking solution, for two hours. The blocking solution also served as the diluent for the primary and secondary antibodies. Following blocking, sections were incubated with guinea pig anti-SubP antibody diluted to 6.25 μg/ml for 40 hrs at 4°C. After several washes, the sections were incubated in the secondary antibody at a concentration of 4.0 μg/ml for 1 hour. The sections were further processed using the ABC Elite kit and ImmPACT DAB (Vector Laboratories, Burlingame, CA) according to the manufacturer's protocol, with one modification. The ImmPACT DAB

solution was diluted 1:1 with ImmPACT DAB diluent, and the optimal time for reaction was determined by staining a test tissue section. Once optimal staining time was determined for each cohort, all of the tissues were stained in the diluted ImmPACT DAB solution for the same length of time. After staining, the reaction was stopped with distilled water; the sections were washed with 0.1 M PBS pH 7.4, mounted onto glass slides, and dried overnight at room temperature. The sections were then cleared in xylenes and coverslips were mounted with DPX mounting medium (VWR International, Poole, England).

Quantification of SubP immunoreactivity—As described previously, the RVM extends from the rostral pole of the inferior olive and the beginning of the VII motor nucleus to the caudal pole of the trapezoid body (Leong et al., 2011). For this study, five to six 50-μm coronal sections spanning the rostral–caudal extent of the RVM were obtained for each rat in the six treatment groups. The optical fractionator probe of Stereoinvestigator software (Microbrightfield Bioscience, Colchester, VT) was used to randomly sample the regions of interest within the RVM as previously described (Hamity et al., 2014). Briefly, a rectangle was centered over the RVM with the top edge aligned with the dorsal edge of the facial nucleus, the base at the dorsal edge of the pyramidal tracts and the lateral edges aligned with the lateral edge of the pyramids. The rectangle was divided along the RVM midline into ipsilateral and contralateral halves, with respect to the injected hindpaw. A virtual grid was used to divide each half of the RVM into 10 regions. Images were obtained from three randomly selected regions (out of the possible 10 regions) on each side, using a Nikon E800 epifluorescence microscope equipped with a Nikon 40X oil Planapoachromat lens (N.A. 1.3). Identical camera settings were used for all images within a cohort. Overall, 15-18 regions within the ipsilateral and 15-18 regions from the contralateral side of the RVM were sampled in a total of five to six sections in each rat.

For quantification, Metamorph software (Molecular Devices, Sunnyvale, CA) was used to binarize SubP immunoreactivity in each image of the RVM. To begin, six immunoreactive processes were randomly selected in each image and the pixel intensity (e.g. 0-255 on a standard grayscale, with 0 = black and 255 = white) was measured. The mean and standard deviation of these six values were calculated. The inclusive threshold function of Metamorph was then used to identify all immunoreactive processes whose intensity fell within the range of the mean and three standard deviations to ensure unbiased measurement of different intensities of Sub P immunoreactivity. The image was then binarized into labeled and unlabeled structures, and the total number of pixels that were defined as immunoreactive was then determined by the Metamorph software program. The 15-18 values from each side of the RVM were averaged to give a single value for each rat. The value for each CFA-treated rat was normalized to the corresponding ipsilateral or contralateral side of its saline-treated cohort. These values were then averaged for each treatment group. All quantification was done by investigators blinded to the treatment condition.

Matrix Assisted Laser Desorption/Ionization-Time of Flight (MALDI-TOF) mass spectrometry

Four day saline- and CFA-treated rats were euthanized with CO_2, exsanguinated, and the brains were quickly removed and placed on ice. L4 and L5 segments of the spinal cord were dissected as a unit on ice after tracing the location of the segment from the innervation of the corresponding nerves. The spinal cord segment was divided into quadrants, and the ipsilateral and contralateral dorsal horn tissue from each side was collected. RVM tissue was dissected as triangles from a 2-mm coronal section of the brainstem, 3-5 mm rostral to the obex. The apex of the triangle was at the fourth ventricle at the midline and the base extended between the lateral edges of the pyramids. The triangles of RVM tissue were also divided into ipsilateral and contralateral halves. Punches of ipsilateral and contralateral PAG were obtained as previously described. Dorsal horn, RVM and PAG tissue were weighed and mechanically homogenized in 0.5 ml of ice cold 2 M acetic acid on ice using a modification of the method described by Savard et al. (1983). The homogenates were centrifuged at 16,100 *g* for 10 min using an Eppendorf 5415r tabletop centrifuge. The supernatant containing both proteins and neuropeptides was carefully removed and filtered using an Amicon Ultra-0.5 centrifugal filter unit with a 10,000 nominal molecular weight cutoff (Millipore, Billerica, MA) by spinning at 14,000 *g* for 45 min at 4°C. The filtrate, containing the low molecular weight peptides, was submitted to the University of Iowa Proteomics Core Facility for analysis by MALDI-TOF mass spectrometry. For samples that were spiked with HK-1, 50 pmoles of peptide were added to 250 μl of the 16,100 *g* supernatant prior to filtration with the Amicon centrifugal filter unit.

The peptide-containing filtrates were concentrated from 250 μl to approximately 10 μl in a speed vacuum for 30 min at room temperature. One μl of the concentrated filtrate was mixed thoroughly with 1 μl of supernatant from saturated α-cyano-4-hydroxycinnamic acid in 50% acetonitrile 0.2% trifluoroacetic acid and spotted on to a MTP 384 well Anchor Chip MALDI plate with hydrophilic centers of 0.8 mm (Bruker, Billerica, MA). Desalting *in situ* was performed by rinsing each dried spot with 3 μl of 0.1% TFA for 20 sec.

SubP, HK-1, trifluoroacetic acid, and α-cyano-4-hydroxysuccinnamic acid (CHCA) were purchased from Sigma (St. Louis, MO). All solutions used with the samples for mass spectrometry analysis were made with water from Burdick and Jackson (Muskegon, MI). Standard solutions used for semi-quantification of SubP and HK-1 were prepared from 1 pmol/μl stock solutions dissolved in 0.1% trifluoroacetic acid. Mass calibration solutions were prepared from Michrom bovine serum albumin digests (Bruker, Billerica, MA). Fourteen peptides ranging in m/z from 927.495 (Tyr-Leu-Tyr-Glu-Ile-Ala-Arg) to 2615.123 (Val-His-Lys-Glu-Cys-Cys-His-Gly-Asp-Leu-Leu-Glu-Cys-Ala-Asp-Asp-Arg-Ala-Asp-Leu-Ala-Lys), with carboxymethylcysteine as a global modification, established a mass accuracy of 4 ppm. SubP and HK-1 were detected in tissue homogenates as well resolved isotope patterns with monoisotopic masses of 1347.68 and 1413.69, respectively.

MALDI-TOF spectra were acquired with a Bruker Autoflex III TOF/TOF mass spectrometer (Billerica, MA) initially floating the source at a homogeneous 25000 V positive bias. Following each laser pulse, a delay of 120 nsec transpired before the bias of

the second lens was dropped to 22,325 V to extract ions. Ions below 730 Da were electronically deflected out of the beam line. Ions traversed an Einsel lens held at 11.9 kV and a two-stage, grid-free reflectron with mid mirror voltage of 13.6 kV and back mirror voltage of 26.45 kV. The laser is a SmartBeam II usually run at 75% attenuation from 200 to 2000 Hz with a laser spot diameter of 60 μm. Mass spectral data were generated by summing 3000-6000 laser shots.

Statistical Analysis

All data were expressed as mean ± SEM. Levels of SubP were compared between saline- and CFA-treated rats using a two-way ANOVA in which one factor was treatment and the other factor was time (four hours, four days, or two weeks). The same analysis was conducted for tissue weights. An unpaired t-test was used to determine whether the levels of mRNA in the RVM differed between saline- and CFA-treated groups. A two-way ANOVA was used to determine whether the levels of mRNA in the PAG differed between sides and treatment group. For analysis of SubP immunoreactivity, a one-sample t-test was used to determine whether the fold-change in CFA-treated rats was significantly different from 1. $P < 0.05$ was considered significant for all analyses.

RESULTS

MALDI-TOF mass spectrometry analysis demonstrates that SubP, but not HK-1, is present in the RVM, PAG and dorsal horn of the spinal cord

These studies employed MALDI-TOF mass spectrometry to clarify whether our samples contained SubP or HK-1. SubP and HK-1 protein can be individually measured and resolved by MALDI-TOF mass spectrometry because of their different ionic masses. Standard solutions of SubP and HK-1 were resolved at 1.0 fmol (Fig. 1A). By diluting the standard solutions of SubP and HK-1, 1.0 atto mole was empirically determined as the limit of detection by MALDI-TOF mass spectrometry.

SubP was detected in all 32 samples examined, which included six extracts each of the RVM and dorsal horn and four extracts of the PAG from naïve rats, as well as six extracts each of the RVM and dorsal horn and four extracts of the PAG obtained from rats four days after CFA treatment. Of these 32 samples, a trace amount of HK-1 was detected in only one and that was in an extract of the RVM from a naïve rat. Figure 1 contains representative spectra from extracts of the RVM (Fig. 1B), PAG (Fig. 1C) and dorsal horn (Fig. 1D) demonstrating the presence of SubP and absence of HK-1. To control for possible degradation or selective removal of HK-1 during sample preparation, 50 pmol of HK-1 was added to homogenates of the RVM and spinal cord at the outset of tissue preparation. Hemokinin-1 was readily detected in these samples (Fig. 1E). Thus, had HK-1 been present in the RVM, PAG or dorsal horn at or above 7 ng/mg tissue, it would have been detected by MALDI-TOF mass spectrometry.

Heat hyperalgesia and inflammation

Rats that received an intraplantar injection of CFA had significant heat hyperalgesia in the ipsilateral hindpaw at four hours, four days, and two weeks compared to saline-treated rats

at each of the corresponding time points ($P < 0.01$ for all groups, data not shown). The PWL of the contralateral hindpaws of saline- and CFA-treated rats did not differ. The thickness of the ipsilateral hindpaw of CFA-treated rats was significantly increased, whereas the contralateral hindpaw of CFA-treated and saline-treated rats did not differ at any time point (data not shown).

Quantitative PCR analysis for *Tac1* and *Tac4* mRNA in the RVM and PAG

Tac1 transcript was readily detected in 5 ng of cDNA from RVM tissue with a mean of 27,216 ± 4,158 (n=14) copy numbers in saline-treated rats, which did not differ from values in naïve rats (31,333 ± 5,159; n=9, P > 0.5). Figure 2 illustrates the levels of *Tac1* mRNA, normalized to *Actb*, in the RVM of saline- and CFA-treated rats at four days and two weeks. The levels of *Tac1* transcript did not differ in saline- and CFA-treated rats either at four days ($P > 0.3$) or two weeks ($P > 0.7$). Levels of *Tac1* mRNAin the RVM of CFA-treated animals in the two week treatment group differed from values from the four day treatment groups (P = 0.04). This difference is most likely the result of slightly lower levels in the four day CFA treatment group. It is unlikely to reflect an increase in levels in the two week treatment group given that neither CFA-treatment group differed from its corresponding, temporally-matched saline-treated control group.

Similarly high levels of *Tac1* transcript were detected in 5 ng of cDNA from PAG tissue of saline-treated rats (34,073 ± 2,492 copy numbers; n = 14). Figure 2B illustrates that levels of *Tac1* transcripts in the ipsilateral and contralateral PAG of CFA-treated rats did not differ from those of their corresponding saline-treated controls either four days or two weeks (P > 0.6, each side) after injection.

Tac4 mRNA was detected at single digit copy numbers. The number of *Tac4* transcripts determined in 5 ng of cDNA prepared from the RVM four days after saline or CFA were 3.7 ± 0.8 (n = 4) and 4.3 ± 1.1 (n = 4), respectively (P > 0.7). Similarly small copy numbers (range: 2.5 – 6) were determined in 5 ng of cDNA of RVM tissue from rats injected two weeks earlier with saline (n = 2) or with CFA (n = 2; data not shown). Preliminary analyses of *Tac4* mRNA levels in two samples of cDNA from PAG tissue indicated that extremely low quantities were present in that region as well.

Total SubP content in homogenates of the RVM, and the PAG and cuneiform nuclei

The RVM was divided into ipsilateral and contralateral sides for analysis. This decision was based on the ontology of serotonergic neurons in the RVM, which arise as separate groups on either side of the floor plate at E14-15 and fuse at the midline by P6 (Levitt and Moore, 1978; Wallace and Lauder, 1983). In addition, we previously observed that the number of neurons expressing NK1R in the RVM was further increased contralateral to the inflamed hindpaw (Hamity et al., 2014), while Leong et al (2011) showed that unilateral spinal nerve ligation caused a preferential loss of neurons in the ipsilateral RVM. The levels of SubP in either the ipsilateral, contralateral, or the combination of both sides of the RVM of CFA-treated rats did not significantly differ from those in corresponding saline-treated rats at any time point (Fig. 3 upper panels).

In contrast to the RVM, CFA treatment induced a time-dependent increase in SubP content in the PAG and cuneiform nuclei. Substance P content in CFA-treated rats did not differ from values in saline-treated rats at four hrs or two weeks (Fig. 3 lower panels). However, at four days after injury, SubP content in CFA-treated rats was increased by nearly two-fold in the PAG and cuneiform nuclei ($P = 0.01$). The increase was significant ipsilateral to the injury and for the combination of both sides, but did not achieve statistical significance for the contralateral side.

Immunohistochemical quantification of SubP immunoreactivity in the RVM after inflammatory injury

Changes in the disposition of SubP, such as increased trafficking to axon terminals or an increased synthesis in a subset of neurons, may be masked when content is determined in tissue homogenates. Therefore, the density of SubP immunoreactivity in the RVM was assessed using immunohistochemistry. Representative photomicrographs of SubP immunoreactivity within the RVM at four hours, four days, and two weeks after saline or CFA treatment are presented in Fig. 4. As expected in the absence of colchicine (Hokfelt et al., 1977), SubP immunoreactivity was confined to puncta and processes in the neuropil and immunoreactive somata were not observed. In agreement with earlier reports, the neuropil of the RVM contained a high density of SubP-immunoreactive puncta, and in the absence of colchicine to block axonal transport (Hokfelt et al., 1977), no immunoreactive somata were observed (Cuello and Kanazawa, 1978; Harmar et al., 1980; Cuello et al., 1982; Harmar and Keen, 1982; Menetrey and Basbaum, 1987).

Quantitative analyses revealed a 2-fold increase in total SubP immunoreactivity (ipsilateral and contralateral sides combined) at four hours in CFA-treated rats compared to saline-treated rats ($P < 0.01$) (Fig. 4I). At four days, SubP immunoreactivity was increased by 2.7-fold in CFA-treated rats ($P < 0.01$). At two weeks, CFA- and saline-treated rats did not differ ($P > 0.2$). Similar increases were observed when the tissue was subdivided into ipsilateral and contralateral RVM.

DISCUSSION

Nerve or inflammatory injury causes a time-dependent increase in SubP expression in the periphery and spinal cord that coincides with increased pain and inflammation (Baranauskas and Nistri, 1998; Sandkuhler et al., 2000; Snijdelaar et al., 2000; Mantyh, 2002; Keeble and Brain, 2004; Seybold, 2009; Todd, 2010; Steinhoff et al., 2014). This study examined whether persistent inflammatory pain similarly alters the content or disposition of SubP in the RVM. It determined that the density of SubP immunoreactive processes and puncta in the RVM increased within four hours and at four days after CFA treatment and returned to basal levels by two weeks. Neither the content of SubP as determined by EIA nor the transcripts for *Tac1* were increased in the RVM of CFA-treated rats. Peripheral inflammatory injury also did not increase transcripts for *Tac1* in the PAG, which contains the cell bodies of SubP-containing neurons that project to the RVM. However, SubP content in the PAG and cuneiform nuclei was increased four days after CFA.

HK-1 is unlikely to play a role in adaptive changes in the RVM after peripheral inflammatory injury

In the midst of these studies, the manufacturer disclosed that the antibody in the commercial EIA kit detects both SubP and HK-1 with 100% fidelity. As noted earlier, the presence of HK-1 was a potential experimental confound because HK-1 has recently been implicated in nociception or itch (Funahashi et al., 2014) and in adjuvant-induced chronic arthritis (Borbely et al., 2013). It is also upregulated in glia by inflammatory stimuli (Morteau et al., 2001; Duffy et al., 2003; Fu et al., 2005; Endo et al., 2006; Matsumura et al., 2008). Levels of *Tac4* in the RVM and PAG were comparable to those reported for the dorsal horn when adjusted for the amount of starting product (Matsumura et al., 2008), confirming prior reports of *Tac4* transcript in the CNS (Kurtz et al., 2002; Duffy et al., 2003). However, MALDI-TOF spectrometry definitively demonstrated that levels of HK-1 in the RVM and the dorsal horn of the spinal cord were negligible in the rat. Moreover, the levels of HK-1 in the RVM or the dorsal horn were not increased following peripheral inflammatory injury. *Tac4* transcript was also not increased in the RVM. These findings confirm that the quantitation of SubP protein with the commercial EIA kit or with immunohistochemistry was likely not confounded by HK-1. They further suggest that HK-1 in the RVM does not contribute to the development of hyperalgesia and mechanical hypersensitivity after peripheral inflammatory injury.

Peripheral inflammatory injury does not increase SubP content but changes its disposition in the RVM

Two approaches were used in concert to examine changes in the content and disposition of SubP in the RVM after inflammatory injury. The first used EIA to quantitate content in homogenates of the RVM. Using this approach, no increase in SubP content was observed on either side of the RVM four hours, four days, or two weeks after CFA treatment. This negative finding was not congruent with the results of earlier pharmacological (Pacharinsak et al., 2008; Hamity et al., 2010; Lagraize et al., 2010), electrophysiological (Budai et al., 2007; Zhang and Hammond, 2009; Brink et al., 2012) and neuroanatomical (Hamity et al., 2014) investigations whose results suggested that CFA treatment may increase SubP release. Measurements in tissue homogenates may not be able to detect small changes in content, changes that are confined to subsets of neurons or changes that occur in specific compartments such as axon terminals. For this reason, an immunohistochemical approach was used as well. These experiments revealed an increase in the density of SubP immunoreactivity in the RVM, localized to processes and puncta, four hours and four days, but not two weeks after CFA.

SubP containing axon terminals and varicosities in the RVM originate from neurons in the nucleus cuneiformis, dorsal raphe nucleus, and PAG (Beitz, 1982; Chen et al., 2013). The most obvious explanation for the increase in SubP immunoreactive processes and puncta in the RVM is an increased synthesis of SubP in PAG and cuneiform neurons. Levels of *Tac1* mRNA in the PAG and cuneiform nuclei were unchanged four days and two weeks after CFA treatment (Fig. 2B). However, SubP content in homogenates of these nuclei was significantly increased four days after CFA. Discordance between mRNA and protein levels is not unknown in the literature (Khositseth et al., 2011; Vogel and Marcotte, 2012; Hamity

et al., 2014). Interestingly, the increased density of immunoreactivity in the RVM preceded the increase in SubP content in the PAG and cuneiform nuclei. Thus, in addition to the obvious explanation that synthesis is increased in the PAG with a concomitant increase in transport to nerve terminals in the RVM, other mechanisms should be considered. For example, it is also possible that SubP, which is diffusely distributed within axons in naïve rats, may redistribute into varicosities in CFA-treated rats where the higher concentration is more readily detected by the antibody. Varicosities may also coalesce and enlarge, similarly making them more readily detected. Finally, this finding could reflect an activity-dependent processing of preprotachykinin to SubP in the axon terminals as has been demonstrated for preprodynorphin in terminals in the CA3 hippocampus or ventral tegmental area (Yakovleva et al., 2006) or to the downregulation of ubiquitin-proteasome mediated protein degradation (Hegde, 2010). Either mechanism could make the axons terminals more readily detected. Although an increase in *Tac1* transcript in the RVM was not observed, changes limited to axons terminals might not have been detectable in the tissue homogenates, which would also contain transcript from SubP containing somata in the RVM that project to the A7 catecholamine nucleus (Yeomans and Proudfit, 1990).

CONCLUSIONS

This study provided the first quantitative determination of SubP levels in the RVM and by quantifying immunostaining provided evidence of increased levels and changes in the disposition of SubP in puncta and processes in the RVM as a consequence of peripheral inflammatory injury. These data, when viewed with our previous report (Hamity et al., 2014) that noxious stimulation increases internalization of the NK1R in CFA-treated rats, provide strong support for an increased release of SubP in the RVM as a consequence of inflammatory injury. The ability of NK1R antagonists to reverse heat hyperalgesia and mechanical hypersensitivity when their actions are confined to the RVM (Pacharinsak et al., 2008; Hamity et al., 2010) implicates this increased release in the development and maintenance of heat hyperalgesia and mechanical hypersensitivity.

Acknowledgements

We thank Dr. Marshall Pope of the University of Iowa Proteomics Facility for interpretations of the MALDI-TOF mass spectrometry data. This work was supported by the National Institutes of Health grants F31NS073250 (U.M.) and R01DA023576 (D.L.H).

Abbreviations

Actb	β-actin
CFA	Complete Freund's adjuvant
C_T	cycle thresholds
EIA	enzyme immunoassay
HK-1	hemokinin-1
MALDI-TOF	matrix assisted laser desorption/ionization-time of flight

Mapk6	mitogen-activated protein kinase 6
NK1R	neurokinin-1 receptor
PAG	periaqueductal gray
PBS	phosphate buffered saline
PWL	paw withdrawal latency
RVM	rostral ventromedial medulla
RT	reverse transcription
SubP	substance P
Tac1	SubP tachykinin
Tac4	HK-1 tachykinin

References

Baranauskas G, Nistri A. Sensitization of pain pathways in the spinal cord: cellular mechanisms. Prog Neurobiol. 1998; 54:349–365. [PubMed: 9481803]

Beitz AJ. The nuclei of origin of brain stem enkephalin and substance P projections to the rodent nucleus raphe magnus. Neuroscience. 1982; 7:2753–2768. [PubMed: 6185878]

Berger A, Paige CJ. Hemokinin-1 has Substance P-like function in U-251 MG astrocytoma cells: a pharmacological and functional study. J Neuroimmunol. 2005; 164:48–56. [PubMed: 15913794]

Borbely E, Hajna Z, Sandor K, Kereskai L, Toth I, Pinter E, Nagy P, Szolcsanyi J, Quinn J, Zimmer A, Stewart J, Paige C, Berger A, Helyes Z. Role of tachykinin 1 and 4 gene-derived neuropeptides and the neurokinin 1 receptor in adjuvant-induced chronic arthritis of the mouse. PLoS One. 2013; 8:e61684. [PubMed: 23626716]

Brink TS, Pacharinsak C, Khasabov SG, Beitz AJ, Simone DA. Differential modulation of neurons in the rostral ventromedial medulla by neurokinin-1 receptors. J Neurophysiol. 2012; 107:1210–1221. [PubMed: 22031765]

Budai D, Khasabov SG, Mantyh PW, Simone DA. NK-1 receptors modulate the excitability of ON cells in the rostral ventromedial medulla. J Neurophysiol. 2007; 97:1388–1395. [PubMed: 17182914]

Camarda V, Rizzi A, Calo G, Guerrini R, Salvadori S, Regoli D. Pharmacological profile of hemokinin 1: a novel member of the tachykinin family. Life Sci. 2002; 71:363–370. [PubMed: 12044836]

Chen T, Wang XL, Qu J, Wang W, Zhang T, Yanagawa Y, Wu SX, Li YQ. Neurokinin-1 receptor-expressing neurons that contain serotonin and gamma-aminobutyric acid in the rat rostroventromedial medulla are involved in pain processing. J Pain. 2013; 14:778–792. [PubMed: 23664790]

Cuello AC, Kanazawa I. The distribution of substance P immunoreactive fibers in the rat central nervous system. J Comp Neurol. 1978; 178:129–156. [PubMed: 344350]

Cuello AC, Priestley JV, Matthews MR. Localization of substance P in neuronal pathways. Ciba Foundation symposium. 1982:55–83. [PubMed: 6183080]

Duffy RA, Hedrick JA, Randolph G, Morgan CA, Cohen-Williams ME, Vassileva G, Lachowicz JE, Laverty M, Maguire M, Shan LS, Gustafson E, Varty GB. Centrally administered hemokinin-1 (HK-1), a neurokinin NK1 receptor agonist, produces substance P-like behavioral effects in mice and gerbils. Neuropharmacology. 2003; 45:242–250. [PubMed: 12842130]

Endo D, Ikeda T, Ishida Y, Yoshioka D, Nishimori T. Effect of intrathecal administration of hemokinin-1 on the withdrawal response to noxious thermal stimulation of the rat hind paw. Neurosci Lett. 2006; 392:114–117. [PubMed: 16229945]

Fu CY, Kong ZQ, Wang KR, Yang Q, Zhai K, Chen Q, Wang R. Effects and mechanisms of supraspinal administration of rat/mouse hemokinin-1, a mammalian tachykinin peptide, on nociception in mice. Brain Res. 2005; 1056:51–58. [PubMed: 16102736]

Funahashi H, Naono-Nakayama R, Ebihara K, Koganemaru G, Kuramashi A, Ikeda T, Nishimori T, Ishida Y. Hemokinin-1 mediates pruriceptive processing in the rat spinal cord. Neuroscience. 2014; 277:206–216. [PubMed: 25016211]

Hahm ET, Hammond DL, Proudfit HK. Substance P induces the reversible formation of varicosities in the dendrites of rat brainstem neurons. Brain Res. 2011; 1369:36–45. [PubMed: 21044613]

Hamity MV, Walder RY, Hammond DL. Increased neuronal expression of neurokinin-1 receptor and stimulus-evoked internalization of the receptor in the rostral ventromedial medulla of the rat after peripheral inflammatory injury. J Comp Neurol. 2014; 522:3037–3051. [PubMed: 24639151]

Hamity MV, White SR, Hammond DL. Effects of neurokinin-1 receptor agonism and antagonism in the rostral ventromedial medulla of rats with acute or persistent inflammatory nociception. Neuroscience. 2010; 165:902–913. [PubMed: 19892001]

Harmar A, Keen P. Synthesis, and central and peripheral axonal transport of substance P in a dorsal root ganglion-nerve preparation in vitro. Brain Res. 1982; 231:379–385. [PubMed: 6173094]

Harmar A, Schofield JG, Keen P. Cycloheximide-sensitive synthesis of substance P by isolated dorsal root ganglia. Nature. 1980; 284:267–269. [PubMed: 6153759]

Hegde AN. The ubiquitin-proteasome pathway and synaptic plasticity. Learn Mem. 2010; 17:314–327. [PubMed: 20566674]

Heinricher MM, Tavares I, Leith JL, Lumb BM. Descending control of nociception: Specificity, recruitment and plasticity. Brain Res Rev. 2009; 60:214–225. [PubMed: 19146877]

Hokfelt T, Ljungdahl A, Terenius L, Elde R, Nilsson G. Immunohistochemical analysis of peptide pathways possibly related to pain and analgesia: enkephalin and substance P. Proc Natl Acad Sci USA. 1977; 74:3081–3085. [PubMed: 331326]

Hurley RW, Hammond DL. The analgesic effects of supraspinal mu and delta opioid receptor agonists are potentiated during persistent inflammation. J Neurosci. 2000; 20:1249–1259. [PubMed: 10648729]

Keeble JE, Brain SD. A role for substance P in arthritis? Neurosci Lett. 2004; 361:176–179. [PubMed: 15135922]

Khasabov SG, Simone DA. Loss of neurons in rostral ventromedial medulla that express neurokinin-1 receptors decreases the development of hyperalgesia. Neuroscience. 2013; 250:151–165. [PubMed: 23831426]

Khositseth S, Pisitkun T, Slentz DH, Wang G, Hoffert JD, Knepper MA, Yu MJ. Quantitative protein and mRNA profiling shows selective post-transcriptional control of protein expression by vasopressin in kidney cells. Mol Cell Proteomics. 2011; 10:M110 004036. [PubMed: 20940332]

Kurtz MM, Wang R, Clements MK, Cascieri MA, Austin CP, Cunningham BR, Chicchi GG, Liu Q. Identification, localization and receptor characterization of novel mammalian substance P-like peptides. Gene. 2002; 296:205–212. [PubMed: 12383518]

Lagraize SC, Guo W, Yang K, Wei F, Ren K, Dubner R. Spinal cord mechanisms mediating behavioral hyperalgesia induced by neurokinin-1 tachykinin receptor activation in the rostral ventromedial medulla. Neuroscience. 2010; 171:1341–1356. [PubMed: 20888891]

Leong ML, Gu M, Speltz-Paiz R, Stahura EI, Mottey N, Steer CJ, Wessendorf M. Neuronal loss in the rostral ventromedial medulla in a rat model of neuropathic pain. J Neurosci. 2011; 31:17028–17039. [PubMed: 22114272]

Levitt P, Moore RY. Developmental organization of raphe serotonin neuron groups in the rat. Anat Embryol (Berl). 1978; 154:241–251. [PubMed: 707816]

Mantyh PW. Neurobiology of substance P and the NK1 receptor. J Clin Psychiatry 63 Suppl. 2002; 11:6–10.

Matsumura T, Sakai A, Nagano M, Sawada M, Suzuki H, Umino M, Suzuki H. Increase in hemokinin-1 mRNA in the spinal cord during the early phase of a neuropathic pain state. Br J Pharmacol. 2008; 155:767–774. [PubMed: 18660829]

Menetrey D, Basbaum AI. The distribution of substance P-, enkephalin- and dynorphin-immunoreactive neurons in the medulla of the rat and their contribution to bulbospinal pathways. Neuroscience. 1987; 23:173–187. [PubMed: 2446203]

Millan MJ. Descending control of pain. Prog Neurobiol. 2002; 66:355–474. [PubMed: 12034378]

Morteau O, Lu B, Gerard C, Gerard NP. Hemokinin 1 is a full agonist at the substance P receptor. Nat Immunol. 2001; 2:1088. [PubMed: 11725292]

Nakaya Y, Kaneko T, Shigemoto R, Nakanishi S, Mizuno N. Immunohistochemical localization of substance P receptor in the central nervous system of the adult rat. J Comp Neurol. 1994; 347:249–274. [PubMed: 7814667]

Pacharinsak C, Khasabov SG, Beitz AJ, Simone DA. NK-1 receptors in the rostral ventromedial medulla contribute to hyperalgesia produced by intraplantar injection of capsaicin. Pain. 2008; 139:34–46. [PubMed: 18407414]

Saffroy M, Beaujouan JC, Torrens Y, Besseyre J, Bergstrom L, Glowinski J. Localization of tachykinin binding sites (NK1, NK2, NK3 ligands) in the rat brain. Peptides. 1988; 9:227–241. [PubMed: 2836823]

Sandkuhler J, Benrath J, Brechtel C, Ruscheweyh R, Heinke B. Synaptic mechanisms of hyperalgesia. Prog Brain Res. 2000; 129:81–100. [PubMed: 11098683]

Savard P, Merand Y, Bedard P, Dussault JH, Dupont A. Comparative effects of neonatal hypothyroidism and euthyroidism on TRH and substance P content of lumbar spinal cord in saline and PCPA-treated rats. Brain Res. 1983; 277:263–268. [PubMed: 6196082]

Seybold VS. The role of peptides in central sensitization. Handb Exp Pharmacol. 2009:451–491. [PubMed: 19655115]

Snijdelaar DG, Dirksen R, Slappendel R, Crul BJ. Substance P. Eur J Pain. 2000; 4:121–135. [PubMed: 10957694]

Steinhoff MS, von Mentzer B, Geppetti P, Pothoulakis C, Bunnett NW. Tachykinins and their receptors: contributions to physiological control and the mechanisms of disease. Physiol Rev. 2014; 94:265–301. [PubMed: 24382888]

Sykes KT, White SR, Hurley RW, Mizoguchi H, Tseng LF, Hammond DL. Mechanisms responsible for the enhanced antinociceptive effects of micro-opioid receptor agonists in the rostral ventromedial medulla of male rats with persistent inflammatory pain. J Pharmacol Exp Ther. 2007; 322:813–821. [PubMed: 17494863]

Todd AJ. Neuronal circuitry for pain processing in the dorsal horn. Nat Rev Neurosci. 2010; 11:823–836. [PubMed: 21068766]

Vogel C, Marcotte EM. Insights into the regulation of protein abundance from proteomic and transcriptomic analyses. Nat Rev Genet. 2012; 13:227–232. [PubMed: 22411467]

Walder RY, Wattiez AS, White SR, Marquez de Prado B, Hamity MV, Hammond DL. Validation of four reference genes for quantitative mRNA expression studies in a rat model of inflammatory injury. Mol Pain. 2014; 10:55. [PubMed: 25187167]

Wallace JA, Lauder JM. Development of the serotonergic system in the rat embryo: an immunocytochemical study. Brain Res Bull. 1983; 10:459–479. [PubMed: 6344960]

Yakovleva T, Bazov I, Cebers G, Marinova Z, Hara Y, Ahmed A, Vlaskovska M, Johansson B, Hochgeschwender U, Singh IN, Bruce-Keller AJ, Hurd YL, Kaneko T, Terenius L, Ekstrom TJ, Hauser KF, Pickel VM, Bakalkin G. Prodynorphin storage and processing in axon terminals and dendrites. FASEB J. 2006; 20:2124–2126. [PubMed: 16966485]

Yeomans DC, Proudfit HK. Projections of substance P-immunoreactive neurons located in the ventromedial medulla to the A7 noradrenergic nucleus of the rat demonstrated using retrograde tracing combined with immunocytochemistry. Brain Res. 1990; 532:329–332. [PubMed: 1704291]

Zhang L, Hammond DL. Substance P enhances excitatory synaptic transmission on spinally projecting neurons in the rostral ventromedial medulla after inflammatory injury. J Neurophysiol. 2009; 102:1139–1151. [PubMed: 19494188]

Highlights

- Peripheral inflammatory injury changes the disposition of Substance P (SubP) in the rostral ventromedial medulla (RVM).
- Levels of SubP and *Tac1* were unchanged in homogenates of the RVM after ipl. injection of CFA; Hemokinin-1 was not detected.
- SubP immunoreactivity in the RVM increased 2 and 2.7-fold four hrs and four days after CFA, and was unchanged at two weeks.
- SubP content in homogenates of the periaqueductal gray, which projects to the RVM, was increased 2-fold four days after CFA.
- These data suggest an increased mobilization and trafficking of SubP to the RVM after injury.

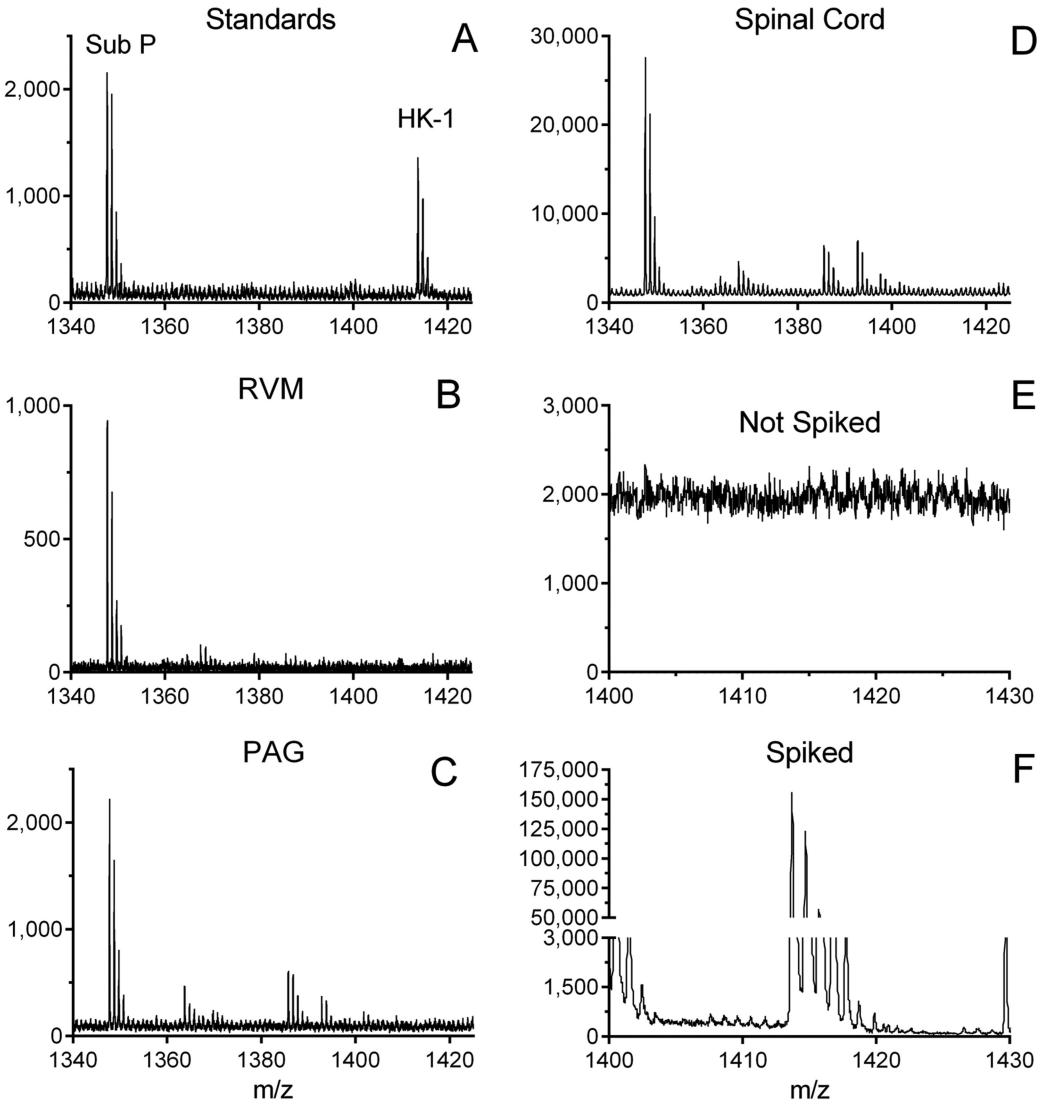

Fig. 1.

MALDI-TOF mass spectra of Substance P (SubP) and hemokinin-1 (HK-1) in the rostral ventromedial medulla (RVM). periaqueductal gray (PAG) and spinal cord of the rat. (A) SubP and HK-1 (1 fmol each) separated with m/z values of 1347.68 and 1413.69, respectively. Representative spectra indicate the presence of SubP and absence of HK-1 in samples of (B) RVM, (C) PAG, and (D) spinal cord. Panels E and F illustrate spectra for a sample from the RVM that was split into two after homogenization, of which one half was spiked with 50 pmol HK-1 prior to further processing. Note that the plate was spotted with an aliquot containing ~ 1 pmol HK-1.

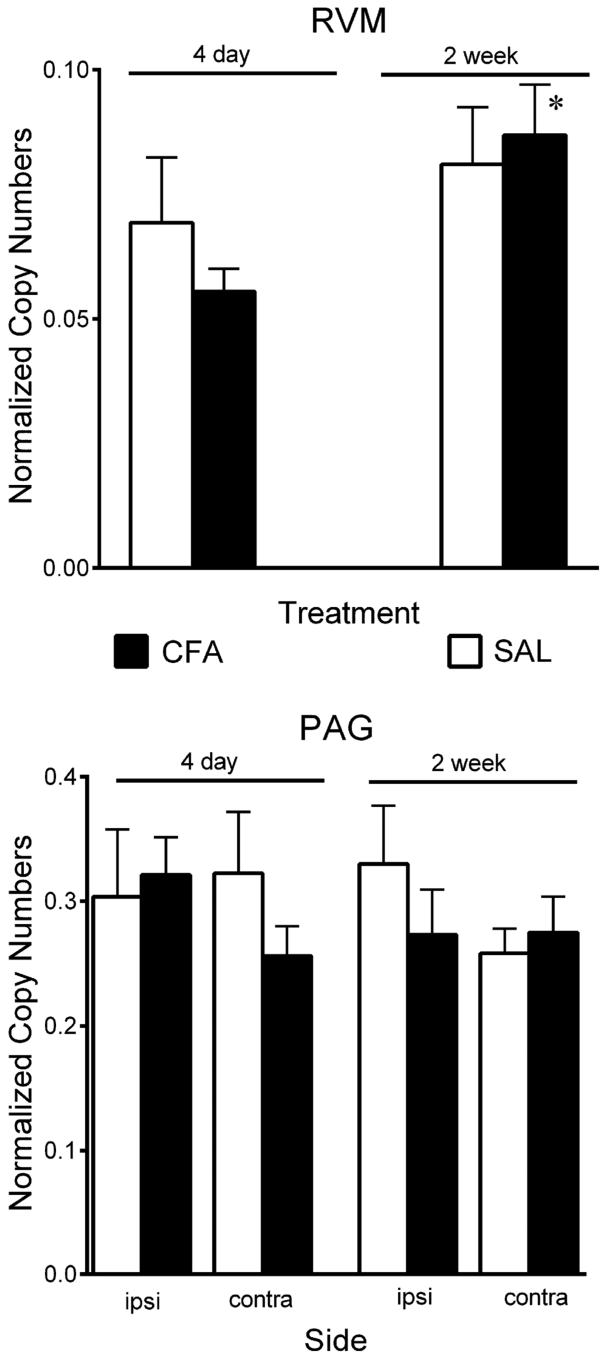

Fig. 2.

Expression of *Tac1* in the rostral ventromedial medulla (RVM) and periaqueductal gray (PAG) of rats does not differ between saline (SAL)- or complete-Freund's adjuvant (CFA)-treated rats either four days or two weeks after intraplantar injection. Experiments for *Tac1* in the RVM were run using 96 well plates and normalized to *Actb*, while those for the PAG were run on 394 well plates and normalized to the geometric mean of *Actb* and *Mapk6*. As a result, the normalized values cannot be compared between regions. Values are the mean ±

S.E.M. of determinations in 6-8 samples. * P = 0.04 compared to four day CFA-treatment group.

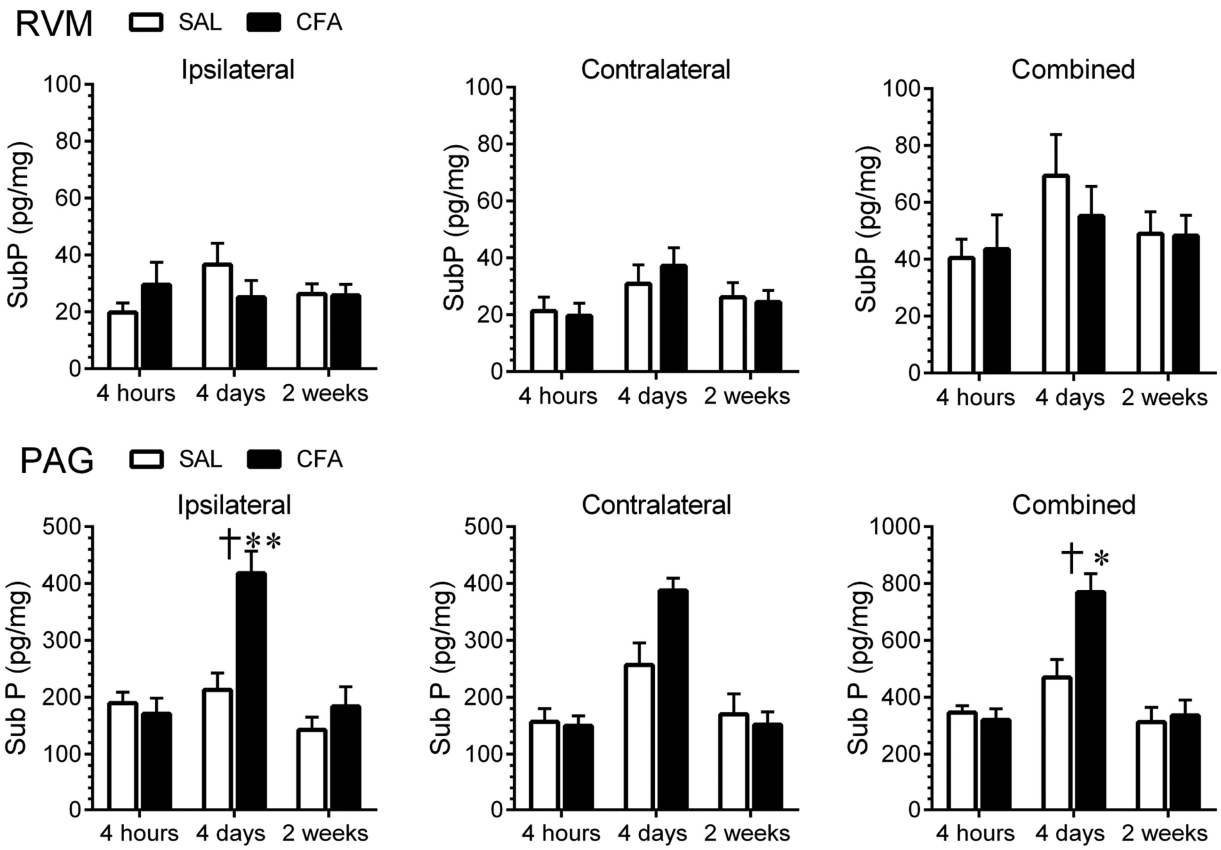

Fig. 3.

Total SubP content as measured by enzyme immunoassay in the rostral ventromedial medulla (upper panels) of rats did not differ between saline (SAL)- or complete Freund's adjuvant (CFA)-treated rats four hours, four days or two weeks after intraplantar injection. In contrast, SubP content increased in the periaqueductal gray and cuneiform nuclei (lower panels) in a time-dependent manner in CFA-treated rats. Values are the mean ± S.E.M. of determinations in 8-15 samples for the RVM and 4-7 for the PAG. * $P < 0.05$, ** $P < 0.01$ compared to saline at the corresponding time point. † $P < 0.05$ compared to CFA-treated rats at 4 hrs or 2 weeks.

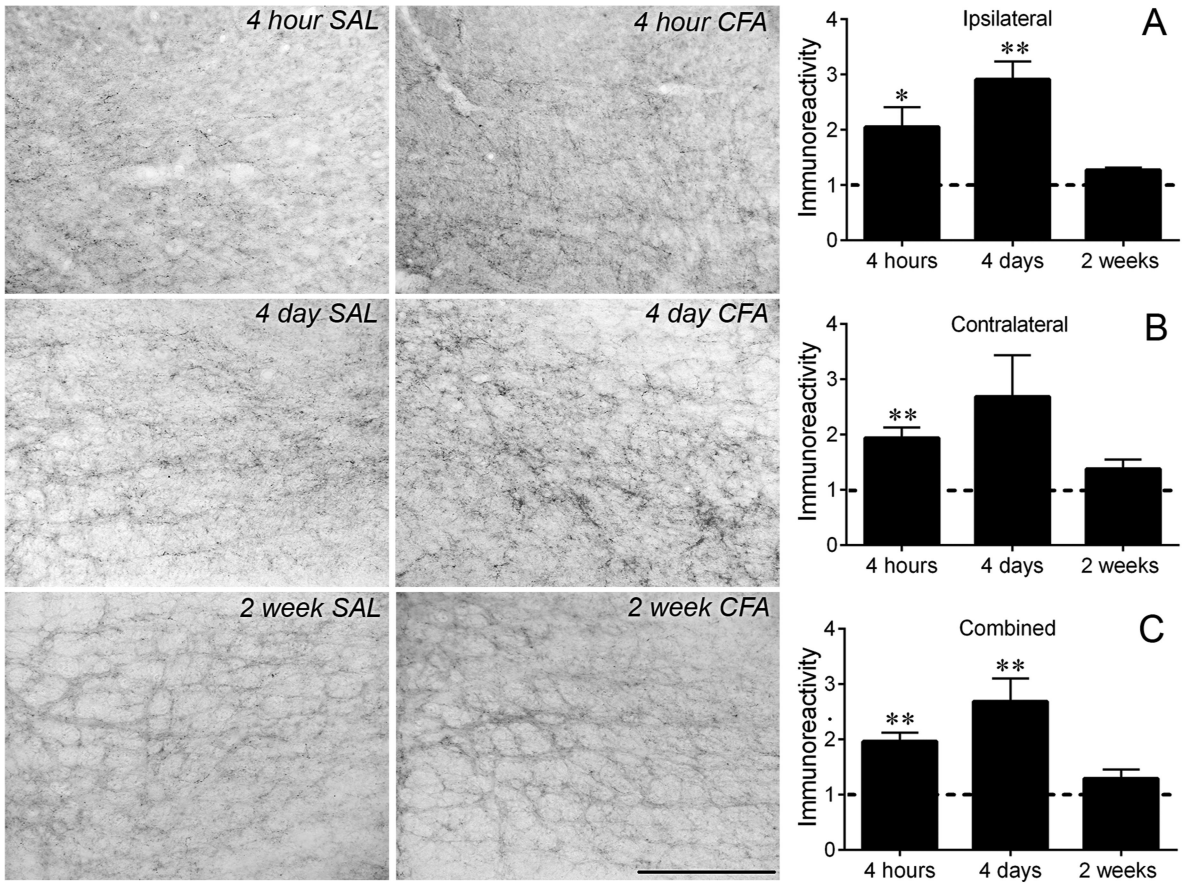

Fig. 4.

Peripheral inflammatory injury increased substance P (SubP) immunoreactivity in the rostral ventromedial medulla (RVM) in a time-dependent manner. Representative images of SubP immunoreactivity in the RVM four hours, four days and two weeks after intraplantar injection of saline or complete Freund's adjuvant (CFA). Scale bar is 200 μm and applies to each image. SubP immunoreactivity in (A) ipsilateral, (B) contralateral and (C) combined RVM increased four hours (n = 5) and four days (n = 6), but not two weeks (n = 3) after intraplantar injection. Data were normalized to the respective ipsilateral, contralateral, or total values in saline-treated rats and expressed as a ratio, where 1 indicates no difference from saline values. Ratios are the mean ± S.E.M. of determinations in 3-6 samples per treatment group. * $P < 0.05$; ** $P < 0.01$ compared to 1 (one-sample t-test).

Table 1

Primer sequences.

Gene Name	Accession Number	Function	Sequence	Product Size (base pairs)
Tac1	Genbank: NM_012666	Substance P tachykinin	*Forward* 5’-GAAATCGGTGCCAACGATGA *Reverse* 5’-GTCTTCGGGCGATTCTCTGA	115
Tac4	Genbank: NM_172328	Hemokinin-1 tachykinin	*Forward* 5’-AGAGGACCTGACTTTCGGTG *Reverse* 5’-GCTTAAGTTCGATGCTGGGG	86
Actb	Genbank: NM_031144	Cytoskeletal structural protein	*Forward* 5’-CCGCGAGTACAACCTTCTTG *Reverse* 5’-GCAGCGATATCGTCATCCAT	81
Mapk6	Genbank: NM_031622	Member of the Ser/Thr protein kinase superfamily	*Forward* 5’-TAAAGCCATTGACATGTGGG *Reverse* 5’-TCGTGCACAACAGGGATAGA	129